Expert Systems With Applications 91 (2018) 434–441

Contents lists available at ScienceDirect

Expert Systems With Applications

journal homepage: www.elsevier.com/locate/eswa

Segmentation of dental X-ray images in medical imaging using neutrosophic orthogonal matrices

Mumtaz Ali[a], Le Hoang Son[b,*], Mohsin Khan[c], Nguyen Thanh Tung[d,e]

[a] University of Southern Queensland 4300, Australia
[b] VNU University of Science, Vietnam National University, Vietnam
[c] Abdul-Wali Khan University, Mardan 23200, Pakistan
[d] VNU International University, Vietnam National University, Vietnam
[e] Nguyen Tat Thanh University, Hochiminh, Vietnam

ARTICLE INFO

Article history:
Received 21 June 2017
Revised 9 September 2017
Accepted 10 September 2017
Available online 12 September 2017

Keywords:
Dental X-ray image
Fuzzy clustering
Neutrosophic orthogonal matrices
Medical diagnosis

ABSTRACT

Over the last few decades, the advance of new technologies in computer equipment, cameras and medical devices became a starting point for the shape of medical imaging systems. Since then, many new medical devices, e.g. the X-Ray machines, computed tomography scans, magnetic resonance imaging, etc., accompanied with operational algorithms inside has contributed greatly to successful diagnose of clinical cases. Enhancing the accuracy of segmentation, which plays an important role in the recognition of disease patterns, has been the focus of various researches in recent years. Segmentation using advanced fuzzy clustering to handle the problems of common boundaries between clusters would tackle many challenges in medical imaging. In this paper, we propose a new fuzzy clustering algorithm based on the neutrosophic orthogonal matrices for segmentation of dental X-Ray images. This algorithm transforms image data into a neutrosophic set and computes the inner products of the cutting matrix of input. Pixels are then segmented by the orthogonal principle to form clusters. The experimental validation on real dental datasets of Hanoi Medical University Hospital, Vietnam showed the superiority of the proposed method against the relevant ones in terms of clustering quality.

1. Introduction

Electronic technology grew remarkably over the last few decades with more powerful computer equipment, cameras and medical devices (Goyal, Beg, & Ahmad, 2017; Kieu, Vo, Le, Deng, & Le, 2017; López, López, de la Torre Díez, Jimeno, & López-Coronado, 2016; Mai, Vo & Nguyen, 2017; Vo, Pham, Le, & Deng, 2017). New medical devices such as the X-ray machines, tomography, magnetic resonance imaging, radiation scans, etc. are present to support professional works of clinicians (Ngan, Tuan, Son, Minh, & Dey, 2016). The on-going development of imaging technology helped to solve many challenges in medical imaging today (Rad, Rahim, & Norouzi, 2014). Medical imaging has made an important contribution to improving the accuracy, timeliness and efficiency of diagnosis (Nowaková, Prílepok, & Snášel, 2017). As based on ultrasound images, physician can accurately measure sizes of typical organ in abdominal cavity (namely liver, spleen, kidneys, pancreas, etc.) and detect abnormal tumors (Setarehdan & Singh, 2012). It helps the physician identify cranial pathologies, especially endoscopic hemorrhoids and brain tumors, and accurately determine abnormalities and masses in the body (Wang et al., 2016).

One of the most crucial tasks in medical imaging is **segmentation,** which divides a medical image into segments for further studies on diseases (Narkhede, 2013). Many algorithms have been developed for the purpose of medical segmentation. The *first approach* is the pixel-based and histogram division method (Nomir & Abdel-Mottaleb, 2005; Rad, Mohd Rahim, Rehman, Altameem, & Saba, 2013; Xu, Xu, Jin, & Song, 2011). The advantages of this method are simple and low in cost, but its disadvantage is sensitivity with threshold values (Rad et al., 2013). The *second approach* is leveling for forward propagation, which is applicable to medical imaging purposes (Bhandari, Kumar, Chaudhary, & Singh, 2016; Dougherty, 2009; Somu, Raman, Kirthivasan, & Sriram, 2016; Zhou & Abdel-Mottaleb, 2005). The advantage of this method is that no complex data structure is used, but it only works when decomposing (Bhandari et al., 2016).

The *last group* - fuzzy clustering divides the data into clusters and determines pixels belonging to those groups (Ayech & Ziou,

* Corresponding author at: 334 Nguyen Trai, Thanh Xuan, Hanoi, Vietnam. Tel.: (+84) 904.171.284.
E-mail addresses: Mumtaz.Ali@usq.edu.au (M. Ali), sonlh@vnu.edu.vn, chinhson2002@gmail.com (L.H. Son), mohsinkhan7284@gmail.com (M. Khan), tungnt@isvnu.vn (N.T. Tung).

http://dx.doi.org/10.1016/j.eswa.2017.09.027
0957-4174/

2015; Bezdek, Ehrlich, & Full, 1984; Son, 2014a,b,c, 2015a,b,c, 2016a,b, Son, Tuan, Fujita, Dey, Ashour, Ngoc& Chu, 2018; Son, Cuong, Lanzi, & Thong, 2012; Son, Cuong, & Long, 2013; Thong & Son, 2015, 2016a,b,c; Tuan, Ngan, & Son, 2016). This algorithm is simple, easy to set up, requiring fair computation complexity; yet the downside is sensitivity to interferences and extraneous elements in the data (Ayech & Ziou, 2015). For instance, some semi-supervised fuzzy clustering frameworks that integrate the spatial constraints and interactive fuzzy satisficing for dental x-ray image segmentation have been presented in Son and Tuan (2016, 2017) and Tuan et al. (2016). So far, there have been some advanced extensions of the fuzzy clustering such as the picture fuzzy clustering, fuzzy geographically weighted clustering, etc., that are likely to apply to the dental x-ray image segmentation (Son, 2014a,b,c, 2015a,b,c, 2016a,b, Son et al., 2012, 2013, 2018; Thong & Son, 2015, 2016a,b,c; Son & Louati, 2016, Son & Thong, 2015, Son & Van Hai, 2016; Son, Wijayanto, & Purwarianti, 2016; Son, Linh, & Long, 2014). Among three groups, the fuzzy clustering group is the most typical one for segmentation of medical images because of its flexibility and adaptability to any kind of images (Nayak, Naik, & Behera, 2015). Nonetheless, it should be further extended on an advanced fuzzy set to gain better representation of medical images (Zhang, Zhang, & Cheng, 2010).

Neutrosophic set (NS) (Smarandache, 2015) is indeed the advanced fuzzy set that is appropriate for such an application. It is defined as a set where each element of the universe has degrees of truth (T), indeterminacy (I) and falsity (F) that lie in the non-standard unit interval, respectively. The uncertainty is the indeterminacy factor which is independent of truth and falsity values while the incorporated uncertainty is dependent on the degrees of belongingness and non-belongingness (Smarandache, 2015). This can handle the problems of sensitivity to interferences and extraneous elements in the data that are remained in the fuzzy clustering (Smarandache, 2015). There are some works that applied neutrosophic approach to image segmentation. Cheng and Guo (2008) regarded an image in the neutrosophic domain including three subsets T, I and F for image thresholding. Guo and Cheng (2009) performed image segmentation using a γ-means clustering. Guo, Cheng, and Zhang (2009) investigated image denoising by the neutrosophic approach. Zhang et al. (2010) employed a watershed algorithm to perform image segmentation in the neutrosophic set. Cheng, Guo, and Zhang (2011) improved Fuzzy C-Means (FCM) on the neutrosophic set for image segmentation with a new α-mean operation for reducing set indeterminacy. There are many works that applied the neutrosophic set for image segmentation; yet they have not been designed for the medical segmentation so far.

In this paper, we aim to **propose a new fuzzy clustering** algorithm for dental x-ray image segmentation based on the neutrosophic set especially the new notion – neutrosophic orthogonal matrix. It converts each pixel of the input image into the neutrosophic sets which are then used to compute the neutrosophic similarity matrix. The cutting matrix is then generated from the neutrosophic similarity matrix which further shapes the clusters of pixels. The new algorithm is validated against the relevant methods with respect to the cluster quality and computation time. Experimental results on real Dental X-Ray datasets (Ngan et al., 2016) confirm the efficiency of the proposal. The new algorithm overcomes disadvantages of the previous algorithms; thereby improving the quality of analysis and diagnosis.

This paper is structured in 5 main sections: Section 1 introduces the content of the article, Section 2 presents preliminary concepts of the neutrosophic set and neutrosophic approaches to image segmentation. Section 3 proposes the clustering method, Section 4 validates it experimentally and lastly Section 5 concludes the paper.

2. Preliminary

2.1. Neutrosophic set

Definition 1. (Smarandache, 2015)**: Neutrosophic Set (NS).**

Let X be a non-empty set and$x \in X$. A neutrosophic set A in X is characterized by a truth membership functionT_A, an indeterminacy membership functionI_A, and a falsehood membership functionF_A. Here, $T_A(x)$, $I_A(x)$ and $F_A(x)$ are real standard or non-standard subsets of $]0^-, 1^+[$ such that T_A,I_A,F_A: $X \to]0^-, 1^+[$. There is no restriction on the sum of $T_A(x),I_A(x)$ and$F_A(x)$, so that $0^- \le T_A(x)+I_A(x)+F_A(x) \le 3^+$. From philosophical point view, the neutrosophic set takes the value from real standard or non-standard subsets of $]0^-, 1^+[$. Thus, it is necessary to take the interval $[0, 1]$ instead of $]0^-, 1^+[$for technical applications because it is difficult to use $]0^-, 1^+[$ in real life applications such as engineering and scientific problems.

If the functions $T_A(x)$, $I_A(x)$ and $F_A(x)$ are singleton subinterval/subsets of the real standard such that $T_A(x)$: $X \to [0, 1]$, $I_A(x)$: $X \to [0, 1]$, $F_A(x)$: $X \to [0, 1]$ then a simplification of the neutrosophic set $A$is denoted by,

$$A = \{(x, T_A(x),\ I_A(x),\ F_A(x)) :\ x \in X\}. \tag{1}$$

with $0 \le T_A(x)+I_A(x)+F_A(x) \le 3$. It is a subclass of neutrosophic set and called simplified neutrosophic set.

Definition 2. (Smarandache, 2015)**:** Let $A_1 = \{\langle x;\ T_1(x);\ I_1(x);\ F_1(x)\rangle | x \in X\}$ and $A_2 = \{\langle x;\ T_2(x);\ I_2(x);\ F_2(x)\rangle | x \in X\}$ be two neutrosophic sets. Some operations on the neutrosophic set are given below:

1. $A_1 \subseteq A_2$ if and only if $T_1(x) \le T_2(x)$; $I_1(x) \ge I_2(x)$; $F_1(x) \ge F_2(x)$,
2. $A_1^c = \{\langle x; F_1(x); I_1(x); T_1(x)\rangle | x \in X\}$,
3. $A_1 \cap A_2 = \{\langle x;\ \min\{T_1(x);\ T_2(x)\};\ max\{I_1(x);\ I_2(x)\};\ max\{F_1(x);\ F_2(x)\}\rangle | x \in X\}$,
4. $A_1 \cup A_2 = \{\langle x;\ \max\{T_1(x);\ T_2(x)\};\ min\{I_1(x);\ I_2(x)\};\ min\{F_1(x);\ F_2(x)\}\rangle | x \in X\}$.

Definition 3. (Smarandache, 2015)**:** Let $V_j (j = 1, 2)$ be two ordinary subsets, and $M \subseteq V_1 \times V_2$ an ordinary relation. Then for any $e, f \in V_2$, $Mf = \{e | eMf\}$ and $eM = \{e | eMf\}$ are respectively called a former set and a latter set.

2.2. Neutrosophic approach to image segmentation

Definition 4. (Cheng & Guo, 2008)**: Neutrosophic Image.**

Let U be a universe of discourse and W be a set included in U, which is composed of bright pixels. A neutrosophic image PNs is characterized by three subsets T, I and F. A pixel P in an image is described as $P(T,\ I,\ F)$ and belongs to W in the following way: it is $t\%$ true in the bright pixel set, $i\%$ indeterminate, and $f\%$ false, where t varies in T, i varies in I, and f varies in F. Each component has a value in $[0, 1]$. Pixel $P(i,\ j)$ in the image domain is transformed into neutrosophic domain: $PNS(i,\ j) = \{T(i,\ j),\ I(i,\ j),\ F(i,\ j)\}$. $T(i,\ j)$, $I(i,\ j)$ and $F(i,\ j)$ represent probabilities belonging to white set, indeterminate set and non-white set, respectively defined as,

$$T(i, j) = \frac{g_{ij} - g_{min}}{g_{max} - g_{min}}, \tag{2}$$

$$I(i, j) = 1 - \frac{H0_{ij} - H0_{min}}{H0_{max} - H0_{min}}, \tag{3}$$

$$F(i, j) = 1 - T(i, j), \tag{4}$$

$$H0(i, j) = |e(i, j)|, \tag{5}$$

where g_{ij} is the pixel value and $H0(i, j)$ is the homogeneity value of T at (i, j), which is described by the local gradient value $e(i, j)$ obtained by using the Sobel operator (Cheng & Guo, 2008).

Besides Definition 4, there were some other definitions of the neutrosophic image published in Cheng et al. (2011), Guo and Cheng (2009), Guo, Cheng, and Zhang (2009) and Zhang et al. (2010). For the analogousness, we only stated the first definitions as above. After transforming an image into the neutrosophic image, some extended operations such as the α-mean and β-enhancement were computed on a subset. K-means or extended FCM algorithm was applied to generate segments according to the achieved values of operations. For more details, please refer to the works of Cheng et al.

3. Neutrosophic clustering based on orthogonal matrix

In this section, we firstly propose the theoretical base for the clustering algorithm in Section 3.1, and then the new neutrosophic clustering algorithm in Section 3.2. This algorithm is different to the neutrosophic approaches for image segmentation of Cheng et al. in terms of using the orthogonal principle to classify objects instead of using operations as in Cheng et al. Specifically, we propose new notions of the neutrosophic relation (Definition 5), the neutrosophic similarity relation (Definition 6), the neutrosophic vector (Definition 7), inner and outer products (Definitions 8 and 9), closeness degree (Definition 10), neutrosophic similarity matrix (Definition 11), cutting matrix (Definition 12), orthogonal neutrosophic matrix (Definition 14) and the orthogonal principle which is used in the clustering algorithm (Definition 15).

The basic idea of the new algorithm is transforming an image into the neutrosophic domain, and then calculating the similarity between pixels expressed in neutrosophic elements. The similarity is stored in the neutrosophic similarity matrix which is used as an input for generation of the cutting matrix. From this, we derive the segments of an image through the orthogonal principle. Details are shown below.

3.1. Theoretical background

Definition 5. Let A and B be two non-empty sets. The following

$$R = \{\langle (a, b), T_R(a, b), I_R(a, b), F_R(a, b)\rangle | a \in A, b \in B\} \quad (6)$$

is called a **neutrosophic relation**, where

$$T_R : A \times B \to [0,\ 1],\ I_R : A \times B \to [0,\ 1], F_R : A \times B \to [0,\ 1] \quad (7)$$

$$0 \le T_R(a, b) + I_R(a, b) + F_R(a, b) \le 3,\ \text{for any } (a, b) \in A \times B. \quad (8)$$

Definition 6. Let A and B be two non-empty sets and R be a neutrosophic relation. If

(a) (Reflexivity). $T_R(a,a)=1,\ I_R(a,a)=0, F_R(a,a)=0$, for any $a \in A$.
(b) (Symmetry). $T_R(a,b) = T_R(b,a),\ I_R(a,b) = I_R(b,a),\ F_R(a,b) = F_R(b,a)$, for any $(a,b) \in A \times B$, then R is called a **neutrosophic similarity relation**.

Definition 7. Let $\alpha = (\alpha_1, \alpha_2, ..., \alpha_n)$ be a vector. If $\alpha_j (j = 1, 2, ..., n)$ are expressed as $(T_{\alpha_j}, I_{\alpha_j}, F_{\alpha_j})$ with $T_{\alpha_j}, I_{\alpha_j}, F_{\alpha_j}$ being the truth, indeterminacy and falsehood membership functions of $\alpha_j$then α is called a **neutrosophic vector**, and α^T denote the transpose of α, where α^T is an $n-$dimensional column vector.

Definition 8. Let A and B be two neutrosophic sets on a universe U. We call

$$A.B = \{u, \langle \vee(T_A(u) \wedge T_B(u)), \wedge(I_A(u) \vee I_B(u)), \wedge(F_A(u) \vee F_B(u))\rangle\} \quad (9)$$

as the **inner product** of A and B, where $\vee$ and $\wedge$ denote the max and min operations, respectively.

Definition 9. Let A and B be two neutrosophic sets on a universe U. The **outer product** of A and B is:

$$A \circ B = \{u, \langle \wedge(T_A(u) \vee T_B(u)), \vee(I_A(u) \vee I_B(u)), \vee(F_A(u) \wedge F_B(u))\rangle\}, \quad (10)$$

where $\vee$ and $\wedge$ denote the max and min operations, respectively.

Theorem 1. *Let α and β be two neutrosophic sets on a universe U. We have*

$$(\alpha \cdot \beta)^C = \alpha^C \circ \beta^C,\ (\alpha \circ \beta)^C = \alpha^C \cdot \beta^C \quad (11)$$

where $\alpha^C = (\alpha_1^C, \alpha_2^C, ..., \alpha_n^C)$, $\beta^C = (\beta_1^C, \beta_2^C, ..., \beta_n^C)$, $\alpha_j^C = (F_{\alpha_j}, I_{\alpha_j}, T_{\alpha_j})$ *and* $\beta_j^C = (F_{\beta_j}, I_{\beta_j}, T_{\beta_j})$, $j = 1, 2, ..., n$. *The symbol 'C'denotes the complement operator stated in Definition 2.*

Proof. According to Definitions 2, 8 and 9, we have

$$\begin{aligned}(\alpha \cdot \beta)^C &= \left(\left(\vee_{j=1}^n \left(T_{\alpha_j} \wedge T_{\beta_j}\right), \wedge_{j=1}^n \left(I_{\alpha_j} \vee I_{\beta_j}\right), \wedge_{j=1}^n \left(F_{\alpha_j} \vee F_{\beta_j}\right)\right)\right)^C \\ &= \left(\wedge_{j=1}^n \left(F_{\alpha_j} \vee F_{\beta_j}\right),\ \wedge_{j=1}^n \left(I_{\alpha_j} \vee I_{\beta_j}\right),\ \vee_{j=1}^n \left(T_{\alpha_j} \wedge T_{\beta_j}\right)\right) \\ &= \alpha^C \circ \beta^C \end{aligned} \quad (12)$$

$$\begin{aligned}(\alpha \circ \beta)^C &= \left(\wedge_{j=1}^n \left(T_{\alpha_j} \vee T_{\beta_j}\right),\ \vee_{j=1}^n \left(I_{\alpha_j} \wedge I_{\beta_j}\right), \vee_{j=1}^n \left(F_{\alpha_j} \vee F_{\beta_j}\right)\right) \\ &= \left(\vee_{j=1}^n \left(F_{\alpha_j} \vee F_{\beta_j}\right), \vee_{j=1}^n \left(I_{\alpha_j} \wedge I_{\beta_j}\right), \wedge_{j=1}^n \left(T_{\alpha_j} \vee T_{\beta_j}\right)\right) \\ &= \alpha^C \cdot \beta^C \end{aligned} \quad (13)$$

□

Theorem 2. *Let α and β be two neutrosophic sets on a universe U. We have*

$$\alpha \cdot \beta = \beta \cdot \alpha, \alpha \circ \beta = \beta \circ \alpha \quad (14)$$

Proof. According to Definitions 8 and 9:

$$\begin{aligned}\alpha \cdot \beta &= \left(max\left\{min\left\{T_{\alpha_j}, T_{\beta_j}\right\}\right\},\ min\left\{max\left\{I_{\alpha_j}, I_{\beta_j}\right\}\right\}, min\left\{max\left\{F_{\alpha_j}, F_{\beta_j}\right\}\right\}\right) \\ &= \left(max\left\{min\left\{T_{\beta_j}, T_{\alpha_j}\right\}\right\},\ min\left\{max\left\{I_{\beta_j}, I_{\alpha_j}\right\}\right\}, min\left\{max\left\{F_{\beta_j}, F_{\alpha_j}\right\}\right\}\right) \\ &= \left(\vee_{j=1}^n \left(T_{\beta_j} \wedge T_{\alpha_j}\right), \wedge_{j=1}^n \left(I_{\beta_j} \vee I_{\alpha_j}\right), \wedge_{j=1}^n \left(F_{\beta_j} \vee F_{\alpha_j}\right)\right) \\ &= \beta \cdot \alpha \end{aligned} \quad (15)$$

$$\begin{aligned}\alpha \circ \beta &= \left(min\left\{max\left\{T_{\alpha_j}, T_{\beta_j}\right\}\right\},\ max\left\{min\left\{I_{\alpha_j}, I_{\beta_j}\right\}\right\}, max\left\{min\left\{F_{\alpha_j}, F_{\beta_j}\right\}\right\}\right) \\ &= \left(min\left\{max\left\{T_{\beta_j}, T_{\alpha_j}\right\}\right\},\ max\left\{min\left\{I_{\beta_j}, I_{\alpha_j}\right\}\right\}, max\left\{min\left\{F_{\beta_j}, F_{\alpha_j}\right\}\right\}\right) \\ &= \left(\wedge_{j=1}^n \left(T_{\beta_j} \vee T_{\alpha_j}\right),\ \vee_{j=1}^n \left(I_{\beta_j} \wedge I_{\alpha_j}\right), \vee_{j=1}^n \left(F_{\beta_j} \vee F_{\alpha_j}\right)\right) \\ &= \beta \circ \alpha \end{aligned} \quad (16)$$

□

Theorem 3. Let $\alpha, \beta, \gamma \in A_{1\times n}$. Then

$$\alpha \cdot (\beta \cdot \gamma) = (\alpha \cdot \beta) \cdot \gamma, \alpha \circ (\beta \circ \gamma) = (\alpha \circ \beta) \circ \gamma \quad (17)$$

Proof. We have

$$\begin{aligned}\alpha \cdot (\beta \cdot \gamma) &= \alpha \cdot (max\{min\{T_{\beta_j}, T_{\gamma_j}\}\},\ min\{max\{I_{\beta_j}, I_{\gamma_j}\}\}, \\ &\quad min\{max\{F_{\beta_j}, F_{\gamma_j}\}\}) \\ &= (max\{min\{T_{\alpha_j}, T_{\beta_j}, T_{\gamma_j}\}\},\ min\{max\{I_{\alpha_j}, I_{\beta_j}, I_{\gamma_j}\}\}, \\ &\quad min\{max\{F_{\alpha_j}, F_{\beta_j}, F_{\gamma_j}\}\}) \\ &= (max\{min\{(T_{\alpha_j}, T_{\beta_j}), T_{\gamma_j}\}\},\ min\{max\{(I_{\alpha_j}, I_{\beta_j}), I_{\gamma_j}\}\}, \\ &\quad min\{max\{(F_{\alpha_j}, F_{\beta_j}), F_{\gamma_j}\}\}) \\ &= (\alpha \cdot \beta) \cdot \gamma \end{aligned} \quad (18)$$

It follows that,

$$\begin{aligned}\alpha \circ (\beta \circ \gamma) &= \alpha \circ (min\{max\{T_{\beta_j}, T_{\gamma_j}\}\},\ max\{min\{I_{\beta_j}, I_{\gamma_j}\}\}, \\ &\quad max\{min\{F_{\beta_j}, F_{\gamma_j}\}\})\end{aligned}$$

$$
\begin{aligned}
&= (min\{max\{T_{\alpha_j}, T_{\beta_j}, T_{\gamma_j}\}\},\ max\{min\{I_{\alpha_j}, I_{\beta_j}, I_{\gamma_j}\}\},\\
&\quad max\{min\{F_{\alpha_j}, F_{\beta_j}, F_{\gamma_j}\}\})\\
&= (min\{max\{(T_{\alpha_j}, T_{\beta_j}), T_{\gamma_j}\}\},\ max\{min\{(I_{\alpha_j}, I_{\beta_j}), I_{\gamma_j}\}\},\\
&\quad max\{min\{(F_{\alpha_j}, F_{\beta_j}), F_{\gamma_j}\}\})\\
&= (\alpha \circ \beta) \circ \gamma \qquad (19)
\end{aligned}
$$

□

Theorem 4. *If α and β are two neutrosophic sets on a universe U then $(\alpha \bullet \beta)$ and $(\alpha \circ \beta)$ are also neutrosophic vectors.*

Definition 10. Let A and B be two neutrosophic sets on U, which is a non-empty universe set. If $R(A, B)$ is a binary relation on $U \times U$

$$R(A,B) = \begin{cases} (1,\ 0),\ A = B \\ (A \cdot B) \cap (A \circ B)^C,\ A \neq B \end{cases} \qquad (20)$$

Then $R(A, B)$ is called the **closeness degree** of A and B.

Theorem 5. *The closeness degree $R(A, B)$ of A and B is a neutrosophic similarity relation.*

Proof.

(1) We first prove that $R(A, B)$ is a neutrosophic vector. Since A and B are two neutrosophic sets on U, we have
(a) *If* $A = B$ then $R(A, B) = (1,\ 0)$,
(b) *If* $A \neq B$ then

$$0 \le T_A(x), I_A(x), F_A(x) \le 1, 0 \le T_A(x) + I_A(x) + F_A(x) \le 3, \qquad (21)$$

$$0 \le T_B(x), I_B(x), F_B(x) \le 1, 0 \le T_B(x) + I_B(x) + F_B(x) \le 3, \qquad (22)$$

$$
\begin{aligned}
(A \circ B)^C = \{&\vee_U (F_A(x) \wedge F_B(x)), \vee_U (I_A(x) \wedge I_B(x)),\\
&\wedge_U (T_A(x) \vee T_B(x))\}
\end{aligned} \qquad (23)
$$

$$
\begin{aligned}
&R(A,B)\\
&= \begin{pmatrix} min\{\wedge_U (T_A(x) \vee T_B(x)), \vee_U (I_A(x) \wedge I_B(x)), \vee_U (F_A(x) \wedge F_B(x))\}, \\ min\{\vee_U (F_A(x) \wedge F_B(x)), \vee_U (I_A(x) \wedge I_B(x)),\ \wedge_U (T_A(x) \vee T_B(x))\} \end{pmatrix}
\end{aligned} \qquad (24)
$$

Thus, $R(A, B)$ is a neutrosophic vector.
(2) Since $R(A, A) = (1,\ 0)$, R is reflexive.
(3) Since $R(A, B) = (A \bullet B) \wedge (A \circ B)^C = (B \bullet A) \wedge (B \circ A)^C = R(B, A)$, R is symmetrical. Thus, $R(A, B)$ is a neutrosophic similarity relation. □

Definition 11. Given A and B be two neutrosophic sets on a universe U and R is a neutrosophic similarity relation. A matrix $M = (r_{pq})_{n \times n}$ is called a **neutrosophic similarity matrix** if $r_{pq} = R(y_p, y_q)$ *where* $p,q = 1,\ 2,\ldots,\ n$ and T_{pq}, I_{pq}, F_{pq} are the truth, indeterminacy and falsehood membership values of an element $(y_p, y_q) \in A \times B$ respectively. Equivalently, $R(y_p, y_q) = (T_{pq}, I_{pq}, F_{pq})$ that implies $r_{pq} = (T_{pq}, I_{pq}, F_{pq})$.

Definition 12. The matrix $(\lambda,\ \delta,\ \tau)M = ((\lambda,\ \delta,\ \tau)r_{ij})_{n \times n} = (\lambda T_{pq}, \delta I_{pq}, \tau F_{pq})_{n \times n}$ is called a $(\lambda,\ \delta,\ \tau)$**-cutting matrix** of M, where $(\lambda,\ \delta,\ \tau)$ is the confidence level, $0 \le \lambda,\ \delta \le 1,\ \tau \le 1,\ 0 \le \lambda + \delta + \tau \le 3$, and

$$
\begin{aligned}
(\lambda,\ \delta, \tau)r_{pq} &= (\lambda T_{pq},\ \delta I_{pq},\ \tau F_{pq})\\
&= \begin{cases} (1,\ 0,\ 0),\ if\ T_{pq} \ge \lambda, I_{pq} \le \delta,\ F_{pq} \le \tau \\ (0,\ 1,\ 0),\ if\ T_{pq} < \lambda, I_{pq} > \delta,\ F_{pq} < \tau \\ (0,\ 0,\ 1),\ if\ T_{pq} < \lambda, I_{pq} < \delta,\ F_{pq} > \tau \end{cases}
\end{aligned} \qquad (25)
$$

Theorem 6. *$M = (r_{pq})_{n \times n}$ is a neutrosophic similarity matrix if and only if its $(\lambda,\ \delta,\ \tau)$-cutting matrix $(\lambda,\ \delta,\ \tau)M = ((\lambda,\ \delta,\ \tau)r_{pq})_{n \times n}$ is a neutrosophic similarity matrix.*

Proof. Suppose that $M = (r_{pq})_{n \times n}$ is a neutrosophic similarity matrix. We gain

(1) (Reflexivity): Since $r_{pp} = (1,\ 0,\ 0)$, $0 \le \lambda,\ \delta \le 1,\ \tau \le 1,\ 0 \le \lambda + \delta + \tau \le 3$, it follows that $(\lambda,\ \delta,\ \tau)r_{pp} = (1,\ 0,\ 0)$.
(2) (Symmetry): Since $r_{pq} = r_{qp}$, i.e., $T_{pq} = T_{qp}, I_{pq} = I_{qp}, F_{pq} = F_{qp}$, from Eq. (24) it follows that $(\lambda,\ \delta,\ \tau)r_{pq} = (\lambda,\ \delta,\ \tau)r_{qp}$.

Conversely, suppose that if$(\lambda,\ \delta,\ \tau)M = ((\lambda,\ \delta,\ \tau)r_{pq})_{n \times n}$ is a neutrosophic similarity matrix then,

(1) (Reflexivity): Since $r_{pp} = (1,\ 0,\ 0)$, for any $0 \le \lambda,\ \delta \le 1,\ \tau \le 1,\ 0 \le \lambda + \delta + \tau \le 3,\ T_{pp} \ge \lambda,\ I_{pp} \le \delta,\ F_{pp} \le \tau$, we have $T_{pp} = 1,\ I_{pp} = 0,\ F_{pp} = 0$, i.e., $r_{pp} = (1,\ 0,\ 0)$.
(2) (Symmetry): If there exists $r_{pq} \neq r_{qp}$, i.e., $T_{pq} \neq T_{qp}, I_{pq} \neq I_{qp}, F_{pq} \neq F_{qp}$, in this case, without loss of generality, suppose that $T_{pq} < T_{qp}$ and let $\lambda = (T_{pq} + T_{qp})/2$, then $T_{pq} < \lambda < T_{qp}$, $\lambda T_{pq} = 0$, $\lambda T_{qp} = 1$. Thus, $(\lambda,\ \delta,\ \tau)r_{pq} \neq (\lambda,\ \delta,\ \tau)r_{qp}$ which contradicts the condition that $(\lambda,\ \delta,\ \tau)r_{pq} = (\lambda,\ \delta,\ \tau)r_{qp}$, for any p, q. Therefore, $M = (r_{pq})_{n \times n}$ is symmetrical.

□

Now, we define the orthogonal matrix as follows.

Definition 13. Let $\alpha,\ \beta \in A$, which is a neutrosophic set. If $\alpha.\beta = (0,\ 1,\ 1)$ or $(0,\ 0,\ 0)$ then α is **orthogonal** to β.

Definition 14. A neutrosophic matrix is called an **orthogonal neutrosophic matrix** if each of its entry is orthogonal to each other.

Definition 15. If we denote $(\lambda, \delta, \tau)\vec{r}_q = ((\lambda, \delta, \tau)r_{1q}, (\lambda, \delta, \tau)r_{2q}, \ldots, (\lambda, \delta, \tau)r_{nq})^T$ as the vector of qth column $(\lambda,\ \delta,\ \tau)M$, then $(\lambda,\ \delta,\ \tau)M = ((\lambda,\ \delta,\ \tau)\vec{r}_1, (\lambda,\ \delta,\ \tau)\vec{r}_2, \ldots, (\lambda,\ \delta,\ \tau)\vec{r}_n)$.

Let $(\lambda,\ \delta,\ \tau)\vec{r}_K, (\lambda,\ \delta,\ \tau)\vec{r}_t$ and $(\lambda,\ \delta,\ \tau)\vec{r}_j (k, t, q = 1, 2, \ldots, n)$ denote the k^{th}, t^{th} and q^{th} column vectors of $(\lambda,\ \delta,\ \tau)R$ respectively. The **orthogonal principle** for clustering neutrosophic information can be classified into the following three categories:

(1) **(Direct clustering principle).** If

$$(\lambda,\ \delta, \tau)\vec{r}_K \cdot (\lambda,\ \delta, \tau)\vec{r}_q = \begin{cases} (1,\ 1, 1) \\ (1,\ 0, 0) \end{cases}, \qquad (26)$$

then $(\lambda,\ \delta, \tau)\vec{r}_K$ and $(\lambda,\ \delta, \tau)\vec{r}_q$ are **non-orthogonal**. In this case, y_k and y_q are clustered into one class.
(2) (**Indirect clustering principle**). If $(\lambda,\ \delta, \tau)\vec{r}_K$ and $(\lambda,\ \delta, \tau)\vec{r}_q$ are non-orthogonal, $(\lambda,\ \delta, \tau)\vec{r}_t$ and $(\lambda,\ \delta, \tau)\vec{r}_q$ are non-orthogonal, then $(\lambda,\ \delta, \tau)\vec{r}_K$ and $(\lambda,\ \delta, \tau)\vec{r}_t$ are non-orthogonal. In this case, y_k and y_q are clustered into one class.
(3) (**Heterogeneous principle**). If

$$(\lambda,\ \delta, \tau)\vec{r}_K \cdot (\lambda,\ \delta, \tau)\vec{r}_q = \begin{cases} (0,\ 1, 1) \\ (0,\ 0, 0) \end{cases} \qquad (27)$$

then $(\lambda,\ \delta, \tau)\vec{r}_K$ is orthogonal to $(\lambda,\ \delta, \tau)\vec{r}_q$. In this case y_k and y_q do not belong to one class.

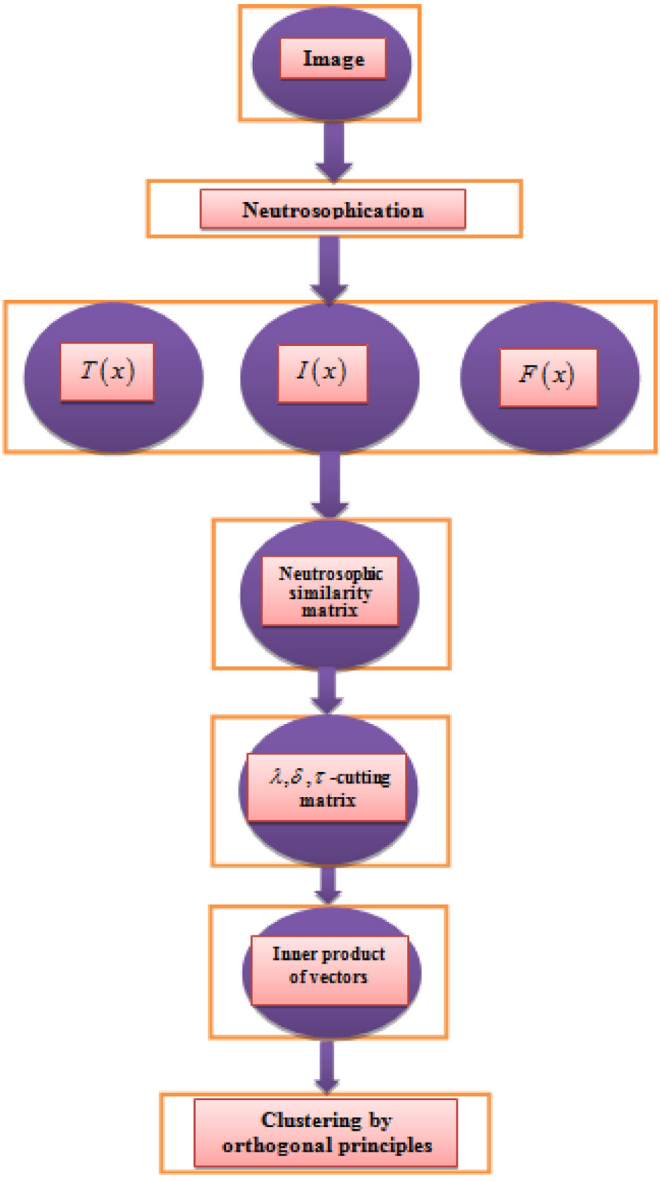

Fig. 1. The CANOM algorithm.

Theorem 7. *If the objects y_k and y_q are clustered into one class by the orthogonal principle under the confidence level $(\lambda_1,\delta_1,\tau_1)$, then we have $\lambda_2 < \lambda_1$, $\delta_2 > \delta_1$, $\tau_2 > \tau_1$, y_k and y_q are still clustered into one class under the confidence level $(\lambda_2,\delta_2,\tau_2)$.*

Proof. Since the objects y_k and y_q are clustered into one class by the orthogonal principle under the confidence level $(\lambda_1,\delta_1,\tau_1)$, two column vectors $(\lambda_1,\delta_1,\tau_1)\vec{r}_K$ and $(\lambda_1,\delta_1,\tau_1)\vec{r}_q$ of $(\lambda_1,\delta_1,\tau_1)-$cutting matrix $(\lambda,\ \delta,\ \tau)R$ are non-orthogonal, i.e., the inner product of $(\lambda_1,\delta_1,\tau_1)\vec{r}_K$ and $(\lambda_1,\delta_1,\tau_1)\vec{r}_q$ is equal to (1, 0) or (1, 1). Suppose that in the p^{th} line, there exist $T_{pk} > \lambda_1$ and $T_{pq} > \lambda_1$. It follows that $\lambda_1 T_{pk} = 1$ and $\lambda_1 T_{pq} = 1$, and if $\lambda_2 < \lambda_1$, $\delta_2 > \delta_1$, $\tau_2 > \tau_1$, $T_{pk} > \lambda_2$ and $T_{pq} > \lambda_2$, then $\lambda_2 T_{pk} = 1$ and $\lambda_2 T_{pq} = 1$ under the confidence level $(\lambda_2,\delta_2,\tau_2)$. Thus, two column vectors $(\lambda_2,\delta_2,\tau_2)\vec{r}_K$ and $(\lambda_2,\delta_2,\tau_2)\vec{r}_q$ are also non-orthogonal, i.e., y_k and y_q are clustered into one class. □

3.2. Neutrosophic clustering

In this section, we present a new neutrosophic clustering algorithm based on the neutrosophic orthogonal matrix for segmentation of a dental X-Ray image. Firstly, we propose the transforming method from a dental image to the neutrosophic domain.

Table 1
Matlab Pseudo-code of the CANOM algorithm.

Input A dental X-Ray image and the confidence level $(\lambda,\ \delta,\ \tau)$
Output Segments of the image
Clustering Algorithm based on Neutrosophic Orthogonal Matrices (CANOM)

```
Read(X_ray_image)
Y = TIF_matrix_of_image
For i = 1 to (row_Y – 1)
  For j = 2 to column_Y
      inner_ product (i, j, 1) = max(min(Y(i, :, 1),Y(j, :, 1)))
      inner_ product (i, j, 2) = min(max(Y(i, :, 2),Y(j, :, 2)))
      inner_ product (i, j, 3) = min(max(Y(i, :, 3),Y(j, :, 3)))
  End
End
For i = 1 to (row_Y – 1)
  For j = 2 to column_Y
       outer_ product (i, j, 1) = max(min(Y(i, :, 3),Y(j, :, 3)))
       outer_ product (i, j, 2) = min(max(Y(i, :, 2),Y(j, :, 2)))
       outer_ product (i, j, 3) = min(max(Y(i, :, 1),Y(j, :, 1)))
  End
End
For i = 1 to row_Y
      For j = 1 to column_Y
          If (i == j)
                similarity_matrix(i, j, 1) = 1
                similarity_matrix(i, j, 2) = 0
                similarity_matrix(i, j, 3) = 0
          else
                similarity_matrix(i, j, 1) = min(inner_ product (i, j,
          1),outer_ product (i, j, 1))
                similarity_matrix(i, j, 2) = max(inner_ product (i, j,
          2),outer_ product (i, j, 2))
                similarity_matrix(i, j, 3) = max(inner_ product (i, j,
          3),outer_ product (i, j, 3))
            End If
      End
End
For i = 1 to row_Y
    For j = 1 to column_Y
      If (similarity_matrix(i, j, 1) >= lamda&&similarity_matrix(i, j,
          2) <= delta &&similarity_matrix(i, j, 3) <= to)
    cutting_matrix(i, j, 1) = 1
    cutting_matrix(i, j, 2) = 0
    cutting_matrix(i, j, 3) = 0
      End If
      If (similarity_matrix(i, j, 1) < lamda&&similarity_matrix(i, j,
          2) > delta &&similarity_matrix(i, j, 3) < to)
    cutting_matrix(i, j, 1) = 0
    cutting_matrix(i, j, 2) = 1
    cutting_matrix(i, j, 3) = 0
          End If
      If (similarity_matrix(i, j, 1) < lamda&&similarity_matrix(i, j,
          2) < delta &&similarity_matrix(i, j, 3) > to)
    cutting_matrix(i, j, 1) = 0
    cutting_matrix(i, j, 2) = 0
    cutting_matrix(i, j, 3) = 1
      End If
    End
End
clust = Calculate_of_cutting_matrix
Data_normal = PCA(clust)
num_clust = numel(unique(clust))
 center_id = findcentroid(clust, Data_normal)
```

Definition 16. The neutrosophication process to convert an image pixel x into the neutrosophic domain is expressed below.

Table 2
Image segmentation of the algorithms.

Image	Original image	FCM	Otsu	eSFCM	CANOM
img_1					
img_2	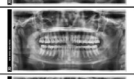		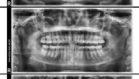		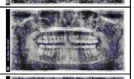
img_3	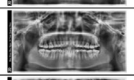	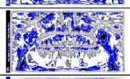			
img_4	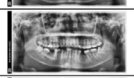	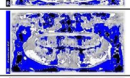	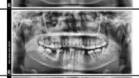		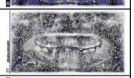
img_5					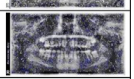
img_6	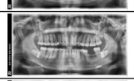				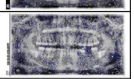
img_7	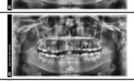	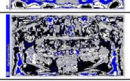			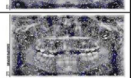
img_8		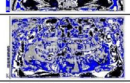	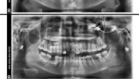		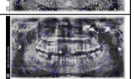
img_9					
img_10					
img_11					
img_12					
img_13					

$$T(x) = \begin{cases} \frac{x-a_1}{a_2-a_1}, & a_1 \le x < a_2, \\ \frac{a_3-x}{a_3-a_2}, & a_2 \le x < a_3, \\ \frac{x-a_3}{a_4-a_3}, & a_3 \le x < a_4 \\ 0, & otherwise. \end{cases}, \quad I(x) = \begin{cases} \frac{b_2-x}{b_2-b_1}, & b_1 \le x < b_2, \\ \frac{x-b_2}{b_3-b_2}, & b_2 \le x < b_3, \\ \frac{b_4-x}{b_4-b_3}, & b_3 \le x < b_4, \\ 1, & otherwise. \end{cases},$$

$$F(x) = \begin{cases} \frac{c_2-x}{c_2-c_1}, & c_1 \le x < c_2, \\ \frac{x-c_2}{c_3}, & c_2 \le x < c_3, \\ \frac{c_4-x}{c_4-c_3}, & c_3 \le x < c_4 \\ 1, & otherwise. \end{cases}, \tag{28}$$

where$a_j \le x \le a_k$ for truth membership, $b_j \le x \le b_k$ for indeterminacy membership and $c_j \le x \le c_k$ for falsehood membership respectively and$j$, $k = 1, 2, 3, 4$. Moreover $T(x)$ is the truth membership, $I(x)$is the indeterminate membership while $F(x)$is the falsehood membership of a pixel in the image domain X. The boundaries points are determined within the ranges of the maximum and minimum values of the dental, background and white parts in a dental X-Ray image (Son & Tuan, 2016).

After having the neutrosophic data, the following pseudo-code is used to derive clusters from a dental image (Table 1).

The following Fig. 1 demonstrates the main activities of the algorithm.

As observed in Table 1 and Fig. 1, the main aim of segmentation is to isolate the basic parts of a dental X-Ray image consisting of the background part, the white part, and the dental part. After completion, the dental part is then given to other processing tools for extraction of patients' states (Son & Tuan, 2016). We employ the orthogonal principle to derive the clusters according to the cutting matrix which is computed from the neutrosophic similarity matrix between pixels. From this, pixels in the boundaries between the background, the white and the dental parts can be determined. For instance, if the truth value of a pixel to the dental is large while the indeterminacy and falsehood membership values are small then we can conclude that it belongs to the dental part. Contrarily, if the indeterminacy value of a pixel is large, it is likely that the pixel is in outliers or white parts. Further procedures are used to derive the final clusters using the orthogonal matrix. This method has benefits of generating confidential results in the application of medical segmentation.

4. Experiments

Based on the real dataset including 66 dental X-ray images from Hanoi Medical University Hospital (Ngan et al., 2016), we validate the CANOM method by validity indices namely DB (Davies & Bouldin, 1979), SSWC (Dougherty, 2009) and VM (Dougherty, 2009) against the Fuzzy C-Means clustering (FCM) (Bezdek et al., 1984), eSFCM (Yin, Shu, & Huang, 2012) and Otsu (1975). The lower value of the Davies–Bouldin (DB), the better an algorithm is. Contrarily, the higher value of the Simplified silhouete width criterion (SSWC), more efficient an algorithm is. Similarly, greater values of IFV and Visibility Metric (VM) would observe better segmentation. The FCM and CANOM methods were run on the Matlab 2016a programming language on a PC with Intel(R) Core (TM) i5 – 3317U CPU @ 1.70 GHz, 4GB RAM, and the operating system was Windows 7 Ultimate 64 bits. The Otsu and eSFCM source codes were taken from (Son & Tuan, 2017) and run again for the experimental data in this research.

Table 3
Comparison of all methods.

	FCM	Otsu	eSFCM	CANOM
DB	18.714	1.832	**0.836**	10.562
SSWC	0.020	0.657	0.647	**0.941**
VM	436.507	N/A	N/A	**484.002**

Table 4
Comparative results in all samples (bold values are the best for a given index).

Image	Algorithm	DB	SSWC	VM	Time (s)
img_1	FCM	15.385	0.020	459.209	**12.128**
	eSFCM	**0.953**	0.762	N/A	16.159
	Otsu	2.33	0.658	N/A	12.754
	CANOM	6.778	**0.961**	**498.177**	13.473
img_2	FCM	20.463	0.020	409.334	10.588
	eSFCM	**0.934**	0.773	N/A	14.121
	Otsu	2.42	0.563	N/A	**10.132**
	CANOM	5.211	**0.941**	**479.179**	15.772
img_3	FCM	21.686	0.020	425.981	10.296
	eSFCM	**0.587**	0.641	N/A	11.112
	Otsu	1.182	0.662	N/A	**9.833**
	CANOM	11.674	**0.959**	**504.991**	12.786
img_4	FCM	19.480	0.020	401.868	**10.103**
img_5	eSFCM	**0.641**	0.698	N/A	11.453
img_6	Otsu	1.417	0.518	N/A	10.217
	CANOM	24.784	**0.911**	**486.313**	13.059
	FCM	15.355	0.020	442.457	**10.443**
	eSFCM	**0.865**	0.864	N/A	12.002
	Otsu	1.982	0.236	N/A	10.862
	CANOM	7.378	**0.946**	**502.822**	13.873
	FCM	17.165	0.020	409.653	11.920
	eSFCM	**0.866**	0.528	N/A	13.951
	Otsu	2.658	0.695	N/A	**9.697**
	CANOM	9.771	**0.941**	**499.874**	14.357
img_7	FCM	18.272	0.020	445.226	11.917
	eSFCM	**0.922**	0.777	N/A	12.172
	Otsu	2.664	0.497	N/A	**10.155**
	CANOM	13.165	**0.931**	**480.030**	14.373
img_8	FCM	24.136	0.020	427.609	**12.883**
	eSFCM	**0.685**	0.657	N/A	13.958
	Otsu	2.233	0.742	N/A	12.994
	CANOM	6.992	**0.960**	**440.404**	14.326
img_9	FCM	16.482	0.020	497.984	11.458
	eSFCM	**0.828**	0.123	N/A	12.862
	Otsu	2.918	0.702	N/A	**10.117**
	CANOM	9.048	**0.928**	**514.140**	14.566
img_10	FCM	21.554	0.020	443.560	**12.350**
	eSFCM	**0.953**	0.654	N/A	13.886
	Otsu	2.341	0.655	N/A	12.742
	CANOM	5.735	**0.941**	**455.979**	15.481
img_11	FCM	17.967	0.020	435.462	**11.790**
	eSFCM	**0.785**	0.746	N/A	12.673
	Otsu	1.476	0.528	N/A	11.791
	CANOM	12.309	**0.914**	**508.220**	13.516
img_12	FCM	16.013	0.020	373.375	11.001
	eSFCM	**0.749**	0.567	N/A	11.542
	Otsu	1.121	0.599	N/A	**10.889**
	CANOM	15.516	**0.938**	**475.644**	13.411
img_13	FCM	19.318	0.020	502.875	10.595
	eSFCM	**0.799**	0.735	N/A	13.190
	Otsu	1.983	0.701	N/A	**9.612**
	CANOM	8.943	**0.959**	**446.257**	13.777
....					

Experimental results: Firstly, intermediate result pictures of the proposed method against some of the related methods are given Table 2. It is obvious that the CANOM method could isolate different regions in the dental X-Ray images. The results on 13 samples show that the results of CANOM are quite stable with most of white, background and the dental parts being isolated clearly (with equivalent membership values *T, I, F*). Contrarily, the FCM produced bad results in some cases with the dental parts being marked as the background or white. This is reflected in Table 2.

In what follows, we compare the results of validity indices of all algorithms in Table 3. The results have demonstrated that the proposed method- CANOM is better than the other algorithms in the SSWC and VM indices whilst in DB, it is not good as the Otsu and eSFCM. The DB index is dependent both on the data as well as the algorithm. Due to the way the index is defined, as a function of the ratio of the within cluster scatter, to the between cluster separation, a lower value means that the clustering is better. In this case the average DB value of CANOM is 10.562 and that of FCM is 18.714. We can see the CANOM DB's index is 43% less than that of FCM. But it is much greater than the Otsu and eSFCM with the values being 1.832 and 0.836. The reason for this fact is that Otsu uses a threshold to divide the clusters (which imply the method is suitable for separation of 2 groups only) and eSFCM utilizes some pre-knowledge in a semi-supervised framework to assist the clustering process. By doing so, the cluster separation is often large and reduces the DB values. On the other hands, the CANOM relies on the neutrosophic orthogonal matrix which further reduces the separation and increases the DB value. It is then understandable that most clustering algorithms deployed on the advanced fuzzy sets often fail into this situation.

Regarding the other validity indices, the CANOM SSWC's index is 0.941 and FCM's SSWC's is 0.02. CANOM is also better than Otsu and eSFCM with the values being 0.657 and 0.647 respectively. The value of CANOM is 47 times larger than that of FCM and 1.43 times larger than those of Otsu and eSFCM. It is known that Simplified silhouete width criterion (SSWC) demonstrates greater value being more efficient algorithm. This index measures how similar an object is to its own cluster compared to other clusters. High value indicates that the object is well matched to its own cluster and poorly matched to neighboring clusters. Thus, we can observe that the proposed CANOM method is better than the relevant algorithm in this index.

The last index – VM can be calculated only with FCM and CANOM. Herein, the proposal CANOM still dominates the best results.

In Table 4, we demonstrate the comparative results of some algorithms in the samples of the dataset. This describes the details of results summarized in Table 3. From this, we still capture the main findings as above. One limitation of CANOM is the running time which is larger than FCM. For instance, the running time of CANOM on the img_1 dataset is 13 seconds whilst that of FCM is 12 seconds. However, the difference and total running time are not much, and the CANOM method is able to run within large datasets.

5. Conclusions

In this paper, we concentrated on the segmentation of medical images using the neutrosophic clustering approach. New notions of neutrosophic orthogonal matrix and related ones have been defined to facilitate the clustering process. The theoretical contributions included the neutrosophic relation, the neutrosophic similarity relation, the neutrosophic vector, inner and outer products, closeness degree, neutrosophic similarity matrix, cutting matrix, orthogonal neutrosophic matrix and the orthogonal principle. These theories are helpful in designing a new clustering algorithm based on the neutrosophic orthogonal matrix which transformed an image into the neutrosophic domain, and calculated the similarity between pixels expressed in neutrosophic elements. The similarity was stored in the neutrosophic similarity matrix which is then used as an input for generation of the cutting matrix. From this, segments of an image are derived through the orthogonal principle.

Experimental results on the real dental X-Ray image datasets have clearly affirmed that the proposed method outperforms the relevant fuzzy clustering scheme. It has been shown that the proposed method achieves better validity index values of DB, SSWC and VM as compared to the Fuzzy C-Means. Some values are bet-

ter than those of Otsu and eSFCM. This facilitates the segmentation of dental X-Ray images in practical applications.

Future research of this work could be conducted on improving the method by an idea of Boole matrix and enhance the computational time by parallel strategy. Recognition of sub-clinical diseases from the achieved segments with context variables and fuzzy solutions as in Cuong, Son, and Chau (2010) and Long, Son, Ha, and Son (2014) is also the next target.

Acknowledgments

The authors would like to send sincere thanks to the National Scientific Study Program, which aims at stable development in the Northwest, for its sponsor to this scientific subject “Applying and Promoting System of Integrated Softwares and Connecting Biomedical Devices with Communications Network to Support Healthcare Delivery and Public Health Epidemiology in the Northwest” (Code number: *KHCN-TB.06C/13-18)*.

References

Ayech, M. W., & Ziou, D. (2015). Segmentation of Terahertz imaging using k-means clustering based on ranked set sampling. *Expert Systems with Applications, 42*(6), 2959–2974.

Bezdek, J. C., Ehrlich, R., & Full, W. (1984). FCM: The fuzzy c-means clustering algorithm. *Computers & Geosciences, 10*(2-3), 191–203.

Bhandari, A. K., Kumar, A., Chaudhary, S., & Singh, G. K. (2016). A novel color image multilevel thresholding based segmentation using nature inspired optimization algorithms. *Expert Systems with Applications, 63*, 112–133.

Cheng, H. D., & Guo, Y. (2008). A new neutrosophic approach to image thresholding. *New Mathematics and Natural Computation, 4*(03), 291–308.

Cheng, H. D., Guo, Y., & Zhang, Y. (2011). A novel image segmentation approach based on neutrosophic set and improved fuzzy c-means algorithm. *New Mathematics and Natural Computation, 7*(01), 155–171.

Cuong, B. C., Son, L. H., & Chau, H. T. M. (2010). Some context fuzzy clustering methods for classification problems. In *Proceedings of the 2010 symposium on information and communication technology* (pp. 34–40). ACM.

Davies, D. L., & Bouldin, D. W. (1979). A cluster separation measure. *IEEE Transactions on Pattern Analysis and Machine Intelligence, 2*, 224–227.

Dougherty, G. (2009). *Digital image processing for medical applications*. Cambridge University Press.

Goyal, L. M., Beg, M. M., & Ahmad, T. (2017). An efficient framework for mining association rules in the distributed databases. *The Computer Journal*, 1–13.

Guo, Y., & Cheng, H. D. (2009). New neutrosophic approach to image segmentation. *Pattern Recognition, 42*(5), 587–595.

Guo, Y., Cheng, H. D., & Zhang, Y. (2009). A new neutrosophic approach to image denoising. *New Mathematics and Natural Computation, 5*(03), 653–662.

Kieu, T., Vo, B., Le, T., Deng, Z. H., & Le, B. (2017). Mining top-k co-occurrence items with sequential pattern. *Expert Systems with Applications, 85*, 123–133.

Long, H. V., Son, N. T. K., Ha, N. T. M., & Son, L. H. (2014). The existence and uniqueness of fuzzy solutions for hyperbolic partial differential equations. *Fuzzy Optimization and Decision Making, 13*(4), 435–462.

López, M. M., López, M. M., de la Torre Díez, I., Jimeno, J. C. P., & López-Coronado, M. (2016). A mobile decision support system for red eye diseases diagnosis: Experience with medical students. *Journal of Medical Systems, 40*(6), 1–10.

Mai, T., Vo, B., & Nguyen, L. T. (2017). A lattice-based approach for mining high utility association rules. *Information Sciences, 399*, 81–97.

Narkhede, H. P. (2013). Review of image segmentation techniques. *International Journal of Modern Engineering, 1*(5461), 28.

Nayak, J., Naik, B., & Behera, H. S. (2015). Fuzzy c-means (FCM) clustering algorithm: a decade review from 2000 to 2014. In *Computational intelligence in data mining-volume 2* (pp. 133–149). India: Springer.

Ngan, T. T., Tuan, T. M., Son, L. H., Minh, N. H., & Dey, N. (2016). Decision making based on fuzzy aggregation operators for medical diagnosis from dental x-ray images. *Journal of Medical Systems, 40*(12), 280.

Nomir, O., & Abdel-Mottaleb, M. (2005). A system for human identification from X-ray dental radiographs. *Pattern Recognition, 38*(8), 1295–1305.

Nowaková, J., Prílepok, M., & Snášel, V. (2017). Medical image retrieval using vector quantization and fuzzy s-tree. *Journal of Medical Systems, 41*(2), 18.

Otsu, N. (1975). A threshold selection method from gray-level histograms. *Automatica, 11*(285-296), 23–27.

Rad, A. E., Rahim, M. S. M., & Norouzi, A. (2014). Level set and morphological operation techniques in application of dental image segmentation. *International Scholarly and Scientific Research & Innovation, 8*(4), 177–180.

Rad, A. E., Mohd Rahim, M. S., Rehman, A., Altameem, A., & Saba, T. (2013). Evaluation of current dental radiographs segmentation approaches in computer-aided applications. *IETE Technical Review, 30*(3), 210–222.

Setarehdan, S. K., & Singh, S. (Eds.). (2012). *Advanced algorithmic approaches to medical image segmentation: State-of-the-art applications in cardiology, neurology, mammography and pathology*. Springer Science & Business Media.

Smarandache, F. (2015). A unifying field in logics: Neutrosophic logic. *Neutrosophic set, neutrosophic probability and statistics*. American Research Press. arXiv: mAth/0101228.

Somu, N., Raman, M. G., Kirthivasan, K., & Sriram, V. S. (2016). Hypergraph based feature selection technique for medical diagnosis. *Journal of Medical Systems, 40*(11), 239.

Son, L. H. (2014a). Enhancing clustering quality of geo-demographic analysis using context fuzzy clustering type-2 and particle swarm optimization. *Applied Soft Computing, 22*, 566–584.

Son, L. H. (2014b). HU-FCF: A hybrid user-based fuzzy collaborative filtering method in recommender Systems. *Expert Systems with Applications: An International Journal, 41*(15), 6861–6870.

Son, L. H. (2014c). Optimizing municipal solid waste collection using chaotic particle swarm optimization in GIS based environments: A case study at Danang City, Vietnam. *Expert Systems with Applications, 41*(18), 8062–8074.

Son, L. H. (2015a). A novel kernel fuzzy clustering algorithm for geo-demographic analysis. *Information Sciences: An International Journal, 317*(C), 202–223.

Son, L. H. (2015b). DPFCM: A Novel distributed picture fuzzy clustering method on picture fuzzy sets. *Expert Systems With Applications, 42*(1), 51–66.

Son, L. H. (2015c). HU-FCF++: A novel hybrid method for the new user cold-start problem in recommender systems. *Engineering Applications of Artificial Intelligence, 41*(C), 207–222.

Son, L. H. (2016a). Dealing with the new user cold-start problem in recommender systems: A comparative review. *Information Systems, 58*, 87–104.

Son, L. H. (2016b). Generalized picture distance measure and applications to picture fuzzy clustering. *Applied Soft Computing, 46*(C), 284–295.

Son, L. H., Tuan, T. M., Fujita, H., Dey, N., Ashour, A. S., Ngoc, V. T. N., & Chu, D. T. (2018). Dental diagnosis from X-Ray images: An expert system based on fuzzy computing. *Biomedical Signal Processing and Control, 39*, 64–73.

Son, L. H., Cuong, B. C., & Long, H. V. (2013). Spatial interaction–modification model and applications to geo-demographic analysis. *Knowledge-Based Systems, 49*, 152–170.

Son, L. H., Cuong, B. C., Lanzi, P. L., & Thong, N. T. (2012). A novel intuitionistic fuzzy clustering method for geo-demographic analysis. *Expert Systems with Applications, 39*(10), 9848–9859.

Son, L. H., Linh, N. D., & Long, H. V. (2014). A lossless DEM compression for fast retrieval method using fuzzy clustering and MANFIS neural network. *Engineering Applications of Artificial Intelligence, 29*, 33–42.

Son, L. H., & Thong, N. T. (2015). Intuitionistic fuzzy recommender systems: An effective tool for medical diagnosis. *Knowledge-Based Systems, 74*, 133–150.

Son, L. H., & Tuan, T. M. (2016). A cooperative semi-supervised fuzzy clustering framework for dental X-ray image segmentation. *Expert Systems with Applications, 46*, 380–393.

Son, L. H., & Van Hai, P. (2016). A novel multiple fuzzy clustering method based on internal clustering validation measures with gradient descent. *International Journal of Fuzzy Systems, 18*(5), 894–903.

Son, L. H., Wijayanto, A. W., & Purwarianti, A. (2016). Fuzzy geographically weighted clustering using artificial bee colony: An efficient geo-demographic analysis algorithm and applications to the analysis of crime behavior in population. *Applied Intelligence, 44*(2), 377–398.

Son, L. H., & Louati, A. (2016). Modeling municipal solid waste collection: A generalized vehicle routing model with multiple transfer stations, gather sites and inhomogeneous vehicles in time windows. *Waste Management, 52*, 34–49.

Son, L. H., & Tuan, T. M. (2017). Dental segmentation from X-ray images using semi–supervised fuzzy clustering with spatial constraints. *Engineering Applications of Artificial Intelligence, 59*, 186–195.

Thong, N. T., & Son, L. H. (2015). HIFCF: An effective hybrid model between picture fuzzy clustering and intuitionistic fuzzy recommender systems for medical diagnosis. *Expert Systems with Applications, 42*(7), 3682–3701.

Thong, P. H., & Son, L. H. (2016a). Picture fuzzy clustering: A new computational intelligence method. *Soft Computing, 20*(9), 3549–3562.

Thong, P. H., & Son, L. H. (2016b). A novel automatic picture fuzzy clustering method based on particle swarm optimization and picture composite cardinality. *Knowledge-Based Systems, 109*, 48–60.

Thong, P. H., & Son, L. H. (2016c). Picture fuzzy clustering for complex data. *Engineering Applications of Artificial Intelligence, 56*, 121–130.

Tuan, T. M., Ngan, T. T., & Son, L. H. (2016). A novel semi-supervised fuzzy clustering method based on interactive fuzzy satisficing for dental x-ray image segmentation. *Applied Intelligence, 45*(2), 402–428.

Vo, B., Pham, S., Le, T., & Deng, Z. H. (2017). A novel approach for mining maximal frequent patterns. *Expert Systems with Applications, 73*, 178–186.

Wang, S., Zhu, X., Zhao, X., Lu, Y., Yang, Z., Qian, X., … Wen, A. (2016). DRUGS system improving the effects of clinical pathways: A systematic study. *Journal of Medical Systems, 40*(3), 40–59.

Xu, X., Xu, S., Jin, L., & Song, E. (2011). Characteristic analysis of Otsu threshold and its applications. *Pattern Recognition Letters, 32*(7), 956–961.

Yin, X., Shu, T., & Huang, Q. (2012). Semi-supervised fuzzy clustering with metric learning and entropy regularization. *Knowledge-Based Systems, 35*, 304–311.

Zhang, M., Zhang, L., & Cheng, H. D. (2010). A neutrosophic approach to image segmentation based on watershed method. *Signal Processing, 90*(5), 1510–1517.

Zhou, J., & Abdel-Mottaleb, M. (2005). A content-based system for human identification based on bitewing dental X-ray images. *Pattern Recognition, 38*(11), 2132–2142.